Cell Reports
Report

Choroid-Plexus-Derived Otx2 Homeoprotein Constrains Adult Cortical Plasticity

Julien Spatazza,[1,5,6] Henry H.C. Lee,[3,5] Ariel A. Di Nardo,[1] Lorenzo Tibaldi,[2] Alain Joliot,[2] Takao K. Hensch,[3,4,*] and Alain Prochiantz[1,*]
[1]Development and Neuropharmacology Group
[2]Homeoprotein Cell Biology Group
College de France, Centre for Interdisciplinary Research in Biology, CNRS UMR 7241, Labex Memolife, PSL Research University, 11 Place Marcelin Berthelot, 75005 Paris, France
[3]FM Kirby Neurobiology Center, Boston Children's Hospital, Harvard Medical School, 300 Longwood Avenue, Boston, MA 02115, USA
[4]Center for Brain Science, Department of Molecular and Cellular Biology, Harvard University, 52 Oxford Street, Cambridge, MA 02138, USA
[5]These authors contributed equally to this work
[6]Present address: Department of Neurological Surgery and The Eli and Edythe Broad Center of Regeneration Medicine and Stem Cell Research, University of California, San Francisco, San Francisco, CA 94143, USA
*Correspondence: hensch@mcb.harvard.edu (T.K.H.), alain.prochiantz@college-de-france.fr (A.P.)
http://dx.doi.org/10.1016/j.celrep.2013.05.014

SUMMARY

Brain plasticity is often restricted to critical periods in early life. Here, we show that a key regulator of this process in the visual cortex, Otx2 homeoprotein, is synthesized and secreted globally from the choroid plexus. Consequently, Otx2 is maintained in selected GABA cells unexpectedly throughout the mature forebrain. Genetic disruption of choroid-expressed *Otx2* impacts these distant circuits and in the primary visual cortex reopens binocular plasticity to restore vision in amblyopic mice. The potential to regulate adult cortical plasticity through the choroid plexus underscores the importance of this structure in brain physiology and offers therapeutic approaches to recovery from a broad range of neurodevelopmental disorders.

INTRODUCTION

Experience shapes neural circuitry during developmental critical periods (CPs) (Hensch, 2004). Thus, cognitive ability is weakened enduringly by adverse environments (Nelson et al., 2007), motor maps reflect early musical training (Elbert et al., 1995), native speech sounds sculpt phonemic perception (Kuhl et al., 1992), and sight strengthens the acuity and connectivity of the two eyes in the primary visual cortex. Imbalanced input ("lazy eye") during this period results in a permanent loss of vision for that eye (Maurer and Hensch, 2012; Prusky and Douglas, 2003), a pathological condition known as amblyopia affecting 2%–4% of the human population. As for many neurodevelopmental disorders, there is currently no cure for amblyopia in adulthood (Bavelier et al., 2010).

Cortical inhibition triggers the onset of the CP of plasticity for binocular vision around postnatal day (P) 21 in mice (Hensch, 2005). Gain- and loss-of-function experiments demonstrate that Otx2 homeoprotein in turn controls the maturational state of a particular subclass of GABAergic interneurons containing parvalbumin (PV) cells (Sugiyama et al., 2008). In *Otx2* heterozygous mice, the visual CP does not open, whereas conversely providing Otx2 protein to wild-type PV cells before P18 opens plasticity ahead of time and anticipates its closure (Sugiyama et al., 2008). The persistent maintenance of Otx2 protein within PV cells throughout life subsequently restricts plasticity levels in adulthood (Beurdeley et al., 2012). Thus, CP timing can be accelerated, delayed, or extended through Otx2 manipulation. Yet, this homeoprotein is neither produced nor confined to the postnatal visual cortex, raising the question as to its origin.

Although the *Otx2* gene is found in several areas of the developing brain, expression in most regions markedly decreases during early ontogenesis (Nothias et al., 1998; Puelles et al., 2004; Rath et al., 2007). A transition from general CNS morphogen to a more narrowly defined role in the pineal gland and retina is suggested (Koike et al., 2007; Rath et al., 2006; Simeone et al., 1993). Indeed, following injection into the eye, exogenous Otx2 is found in visual cortical PV cells, and disrupting intraocular synthesis or its translocation into PV cells impacts visual plasticity (Beurdeley et al., 2012; Sugiyama et al., 2008). But, these findings do not rule out other possible sources of Otx2, during and beyond development. In this study, we demonstrate that the choroid plexus is a global source of Otx2 (Johansson et al., 2013). As a result, knocking down *Otx2* in this structure impairs its transfer into distant PV cell targets and thus allows the reactivation of plasticity in the adult visual cortex. Moreover, a much broader role for Otx2 beyond the visual cortex is suggested.

RESULTS

Otx2 Expression in the Adult Brain and Choroid Plexus

After eye opening, Otx2 homeoprotein is transferred into the primary visual cortex by an activity-dependent mechanism (Sugiyama et al., 2008), thus triggering PV cell maturation and CP opening. Given the widespread distribution of PV cells

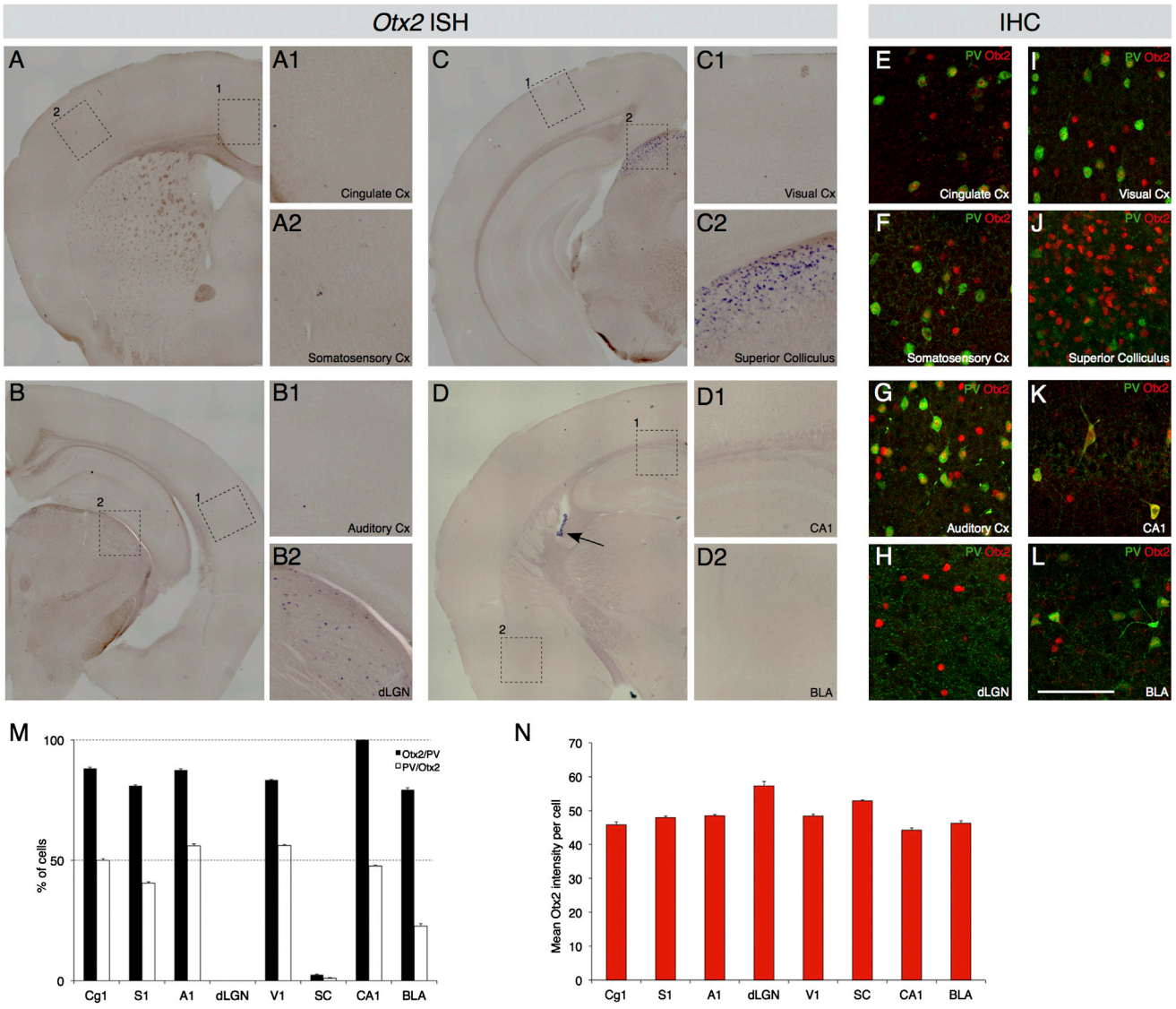

Figure 1. Non-Cell-Autonomous Otx2 Protein Is Localized throughout the Adult Cortex

(A–D) In situ hybridization of *Otx2* mRNA performed on adult wild-type mouse brain coronal sections shows locus activity in the dLGN, SC, and choroid plexus (arrow). Framed regions are magnified and labeled (A1, A2, B1, B2, C1, C2, D1, and D2).

(E–L) Corresponding immunostaining for Otx2 and PV in the regions highlighted in (A)–(D) reveals Otx2 protein where the *Otx2* locus is inactive (scale bar, 100 μm).

(M and N) Quantification of Otx2 colocalization in PV cells and vice versa (M) and of Otx2 immunostaining intensity per cell (N) across brain regions (three mice, five sections each). Error bars, SEM.

A1, auditory cortex; CA1, field of hippocampus; Cg1, cingulate cortex; Cx, cortex; S1, somatosensory cortex; V1, visual cortex.

throughout the forebrain and the presence on their surface of peri-neuronal nets (PNNs) required for Otx2 internalization (Beurdeley et al., 2012; Miyata et al., 2012), we examined whether Otx2 translocation might be a common principle, not solely limited to the visual cortex. We have previously shown, by RT-PCR and with the *Otx2*$^{GFP/+}$ knockin mouse line, that the *Otx2* locus is silent in the visual cortex (Sugiyama et al., 2008). We now confirmed by in situ hybridization that *Otx2* transcripts are not found anywhere throughout the adult cortex (Figures 1A–1D), whereas evident in dorsal thalamus (dorsal lateral geniculate nucleus [dLGN]) and superior colliculus (SC) as expected (Figures 1B2 and 1C2). Interestingly, immunohistochemistry (Figures 1E–1L) revealed Otx2 protein across prefrontal, auditory, somatosensory, and visual cortices as well as limbic structures (basolateral amygdala [BLA], hippocampal CA1).

In all cortical regions where the protein was present but the locus inactive, the vast majority of Otx2-stained cells also expressed PV (Figure 1M). In contrast, in the dLGN and SC where the *Otx2* locus is active, Otx2 was not detected in PV-expressing cells (Figure 1M). In the dLGN, we could not quantify colocalization because PV was present in the neuropil but not in cell bodies. The mean intensity of Otx2 staining per cell was similar

in all regions independent of whether Otx2 activity was cell autonomous or not, even though a slightly higher expression may be seen in the cell-autonomous regions (Figure 1N).

One potential explanation for this widespread distribution of Otx2 could be a global source from which it is secreted. The choroid plexus, an established site of *Otx2* expression (Johansson et al., 2013; Simeone et al., 1993), is a very attractive candidate, known for its intense secretory activity and cerebrospinal fluid (CSF) production (Johanson et al., 2008). The CSF also carries a wide range of signaling molecules acting at the level of the parenchyma. In early development, the choroid plexus provides a niche of proliferative factors (IGF1, FGF2, Shh, retinoic acid) (Alonso et al., 2011; Huang et al., 2010; Lehtinen et al., 2011; Martín et al., 2006) and concentration gradients of guidance molecules for migrating neural adult progenitor cells (Sawamoto et al., 2006). Thus, a similar paracrine release of Otx2 may likewise affect postnatal plasticity by regulating neocortical PV cells.

In situ hybridization on adult brain sections confirmed the expression of *Otx2* in the choroid plexus of the lateral and fourth ventricles (Figures 2A, 2A1, and 2A2), as well as third ventricle (data not shown). We next applied a secretion assay developed for other homeoproteins (Engrailed, Pax6) (Di Lullo et al., 2011; Wizenmann et al., 2009) to choroid plexus dissected from the fourth ventricle of adult mice. The assay based on the biotinylation of cell surface proteins (Figure 2B) demonstrates that around 4.5% of total Otx2 is accessible to the extracellular biotinylation reagent. Accessibility was also true for TrkB, a transmembrane protein, but not for RhoA, a control intracellular protein. Similar results were obtained following the cell surface biotinylation of choroid epithelial cells in culture (data not shown).

We further examined the presence of Otx2 in the CSF. Given its low protein concentration and limited availability in adult mice, CSF was collected from ten adult mice. Transthyretin (TTR), the major thyroid hormone transporter in the CNS, is specifically expressed by the choroid plexus and secreted into the CSF, where it represents ~25% of all proteins (Weisner and Roethig, 1983). Figure 2C reveals the presence of both Otx2 and TTR in the CSF. In contrast, TrkB, also expressed in the choroid plexus (Timmusk et al., 1995), is not detected in the CSF sample (Figure 2C). In Figure 2C, the exposure time for Otx2 and TrkB in the mouse CSF (mCSF) is 60-fold that of the other panels. The absence of membrane-bound protein TrkB in these conditions makes it unlikely that Otx2 in the CSF reflects cellular contamination but, rather, secretion from the choroid plexus. However, it also indicates that Otx2 concentration in the CSF is very scarce and that the protein following its release from the cell surface is likely rapidly transported to the brain parenchyma and from there into PV cells (see Discussion).

Knocking Down *Otx2* in the Choroid Plexus Decreases Its Cortical Content

To probe the putative impact of Otx2 release into the CSF upon cortical function, we developed a loss-of-function technique. A cell-permeable recombinase (CRE-Tat), obtained by the fusion of the bacterial enzyme with a peptide vector, was injected into the lateral ventricles of adult reporter mice (ROSA26R) (Soriano, 1999). The efficiency of recombination tested 5 days after a single injection was very high, as demonstrated by the substantial *LacZ* expression in the choroid plexus (Figures 2D–2F). This access to the choroid plexus was extremely specific as illustrated by the absence of recombination in the dLGN and SC (Figures 2F and 2G). The specificity of CRE-Tat targeting is best explained by the CSF clearance activity of the choroid plexus through rapid apical reabsorption (Johanson et al., 2008).

We next turned to $Otx2^{flox/flox}$ mice (Fossat et al., 2006; Nishida et al., 2003) and waited for 14 days after CRE-Tat injection before assessing the efficiency of *Otx2* deletion at the level of the genome, mRNA, and protein content. Although the genomic rearrangement in the choroid plexus was not complete, it was specific and did not affect the retina, dLGN, or SC (Figure 2H). Accordingly, a strong and specific decrease in both *Otx2* mRNA and protein content (Figure 2I) was observed in the choroid plexus of CRE-Tat-treated animals when compared to vehicle-treated animals (mRNA: vehicle, 1.00 ± 0.056, VS CRE-Tat, 0.36 ± 0.056, $p = 0.022$; protein: vehicle, 1.00 ± 0.065, VS CRE-Tat, 0.24 ± 0.049, $p = 0.028$), whereas these parameters were not significantly different from control in the retina, dLGN, and SC of CRE-Tat-treated animals.

If Otx2 is maintained in adult brain by the choroid plexus, then protein levels in distant cortex should be modified by our CRE-mediated conditional deletion strategy. Indeed, a significant reduction in the number of Otx2-positive cells and their mean fluorescence intensity was observed in the binocular visual cortex (V1b) of CRE-Tat-treated animals compared to vehicle (Figures 3A, 3F, 3K, and 3L; cell number: 68.1% ± 3.7%, $p = 0.002$; mean intensity per cell: vehicle, 100 ± 1.2 versus CRE-Tat, 82.9 ± 1.2, $p = 0.0008$). Consistent with our previous work indicating an Otx2 requirement for PV expression and PNN assembly early in life (Sugiyama et al., 2008), a parallel decrease of PV (Figures 3B, 3G, 3K, and 3L; cell number: 74.1% ± 4.7%, $p = 0.009$; mean intensity per cell: vehicle, 100 ± 1.9 versus CRE-Tat, 91.3 ± 2.0, $p = 0.0013$) and PNN expression (Figures 3C, 3H, and 3K; WFA-positive cell number: 68.5% ± 4.2%; $p = 0.002$) was observed following CRE-Tat injection.

Neither the number of calretinin-positive cells (Figures 3D, 3I, and 3K; 93.9% ± 2.3%; $p > 0.05$) nor their mean intensity (Figure 3L; vehicle, 100 ± 1.5 versus CRE-Tat, 101.7 ± 1.5; $p > 0.4$) was altered, indicating a PV cell-specific effect. In addition, given that the CSF might convey Otx2 more broadly, we checked marker levels in the BLA. In this region, a decrease in Otx2, PV, and PNN staining was observed as early as 4 days after CRE-Tat injection, compared to saline controls (Otx2, 65.4% ± 5.4%, $p = 0.0068$; PV, 66.3% ± 3.1%, $p = 0.0041$; WFA, 77.4% ± 1.0%, $p = 0.0020$; $n = 6$ for each group). This indicates that the kinetics of Otx2 regulation from the choroid plexus may differ by brain region. Importantly, the total number of neurons identified by NeuN staining was not modified in BLA (100.5% ± 9.1%; $p > 0.4$; $n = 6$ for each group) nor that of GABA-stained cells in V1 or the intensity of GABA staining (Figures 3E, 3J, 3K, and 3L; cell number: 100.3% ± 1.3%, $p > 0.4$; intensity: vehicle, 100 ± 2.1 versus CRE-Tat, 100.7 ± 2.1, $p > 0.4$; $n = 8$ for each group), thus discounting the possibility of cell death in both regions.

The decrease of Otx2 in layers III/IV of the visual cortex after recombination in the adult choroid plexus later than P90 is illustrated (western blot) and quantified in Figure 3M. Comparison

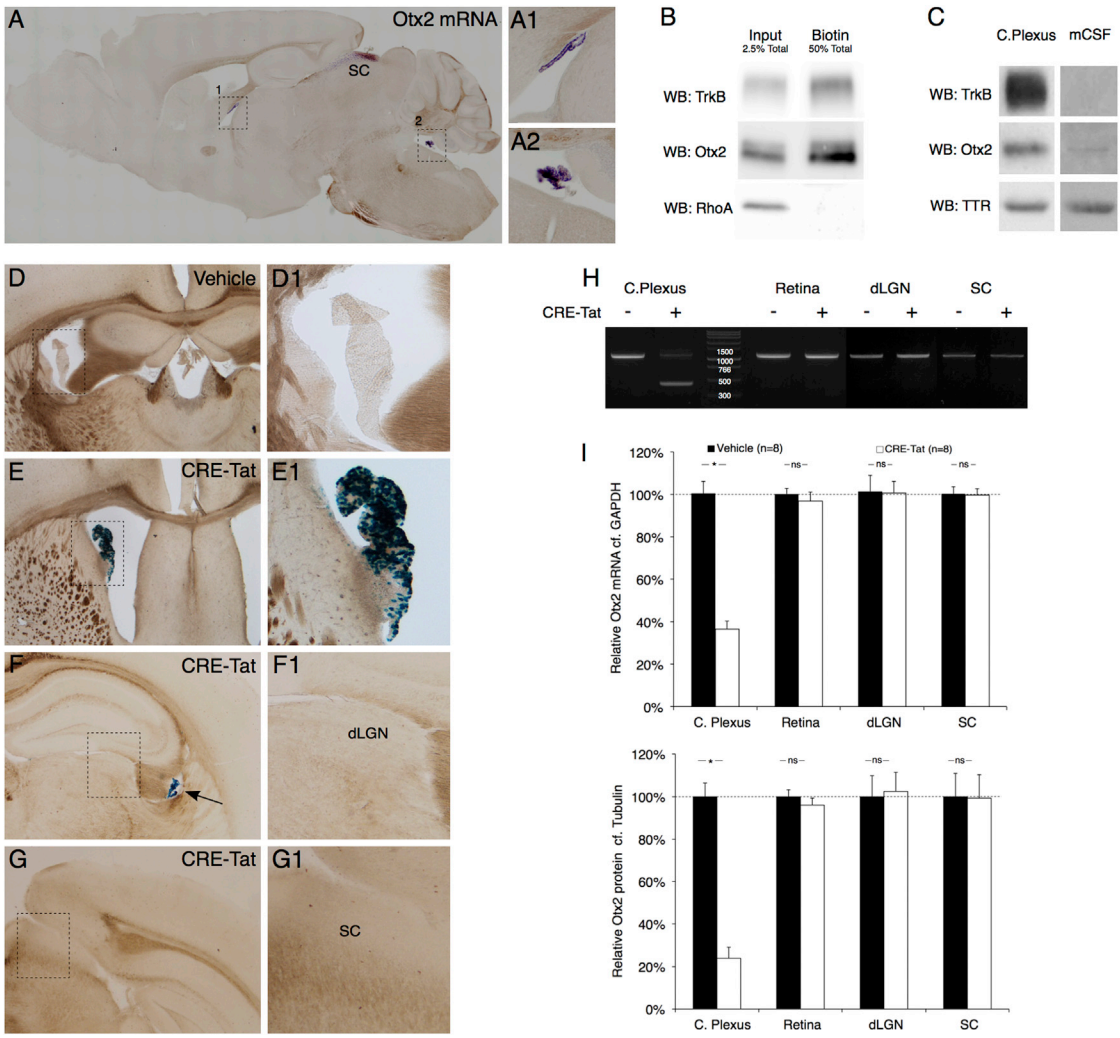

Figure 2. Otx2 Synthesis, Secretion, and Genetic Deletion in the Choroid Plexus

(A) Sagittal brain in situ hybridization reveals *Otx2* expression in adult SC and choroid plexus. Insets show lateral ventricle (A1) and fourth ventricle (A2).

(B) Detection of choroid plexus cell surface proteins with surface biotinylation assay. Inputs show extracellular (TrkB) and intracellular (RhoA) protein. Upon biotinylation of adult choroid plexus, a pool of Otx2 (5% of total) is found to be extracellular (compare TrkB and RhoA). Note that 2.5% of total extracts and 50% of biotinylated fractions were loaded.

(C) Western blots of mouse choroid plexus and CSF protein extracts probed for TrkB (a transmembrane protein), TTR (a protein secreted by the choroid plexus), and Otx2. Only Otx2 and TTR are detected in CSF. Film exposure times for mCSF TrkB and Otx2 boxes are 60-fold longer than for mCSF TTR.

(D–G) X-Gal staining of adult ROSA26R mouse brain sections 5 days after single icv injection of vehicle solution (D) or CRE-Tat protein (E–G) reveals recombination in choroid plexus (E, arrow in F). Framed regions are enlarged (D1, E1, F1, and G1).

(H and I) Recombination in *Otx2*$^{flox/flox}$ mice 14 days after single icv injection of vehicle solution (–) or CRE-Tat protein (+). (H) Genomic DNA extracted from choroid plexus, retina, dLGN, and SC was analyzed by PCR using primers surrounding the flox cassettes (Fossat et al., 2006) yielding an expected 451 bp amplicon upon recombination of the *Otx2* locus. Only the choroid plexus of CRE-Tat-treated animals exhibits partial recombination. (I) Quantification of *Otx2* mRNA and protein content in choroid plexus, retina, dLGN, and SC of vehicle-treated and CRE-Tat-treated animals. Error bars, SEM (Mann-Whitney U test; eight mice per group; *$p < 0.05$).

with the time course of Otx2 accumulation in layer III/IV-containing PV cells (Figure 3N) demonstrates that following recombination, the level of Otx2 is similar to that observed at CP opening (P21). Interestingly, *Otx2* mRNA expression (RT-PCR) by the choroid plexus increased only slightly between P7 and P90 (Figure 3O); a similar pattern was seen for total Otx2 protein (data not shown). This constant expression before and after the visual CP was also seen at the level of surface-associated Otx2 protein (4.6% pre-CP and 5.4% post-CP) as well as for Otx2 in the CSF (Figure 3P), even though the low amounts of protein in the CSF (see above) make quantification difficult. Taken together, these results suggest that the amount of Otx2 in PV cells is not regulated by the levels expressed by the choroid plexus and released into the CSF but, rather, by the ability of the cells to capture the homeoprotein. This conclusion is consistent with previous results demonstrating that PNN assembly regulates Otx2

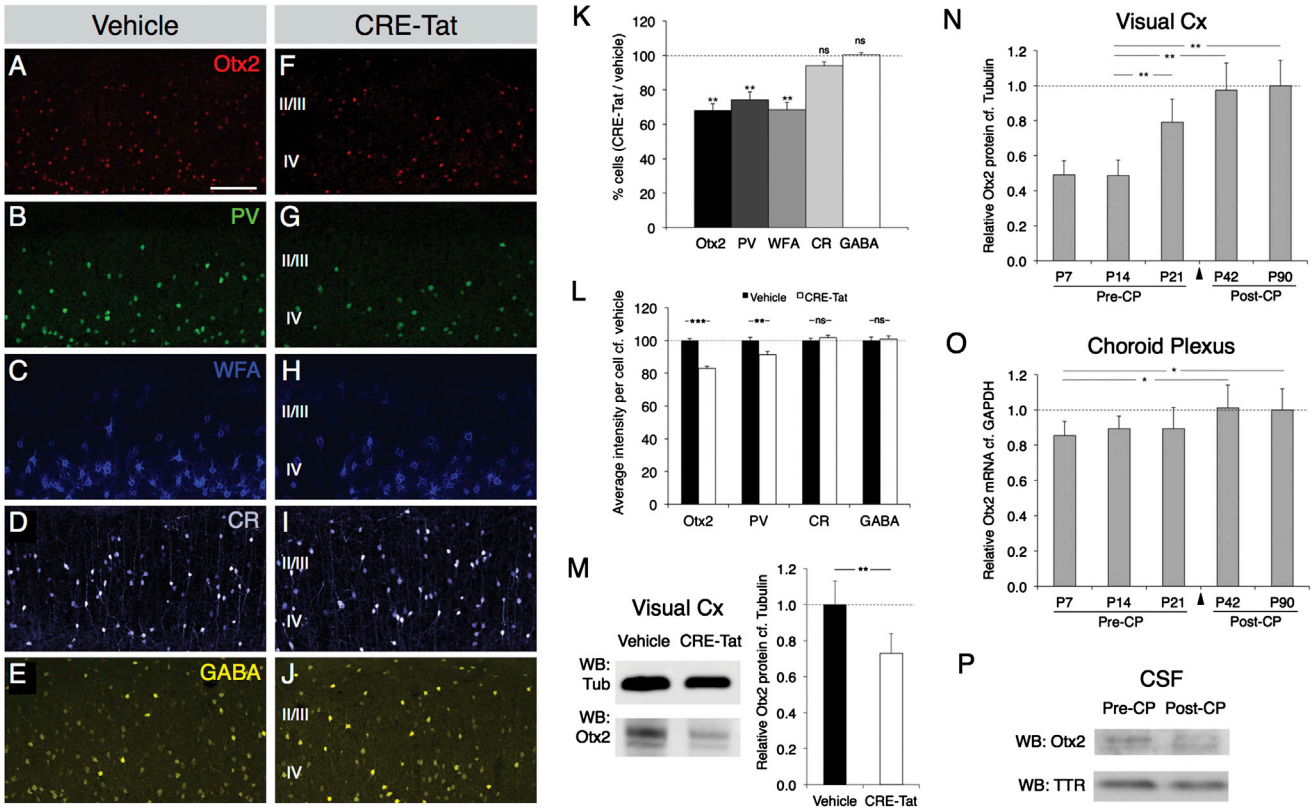

Figure 3. Choroid *Otx2* Disruption Selectively Impacts PV Cells in Visual Cortex

(A–J) Immunostaining for Otx2, PV, WFA, calretinin (CR), and GABA in layers II–IV of V1b from adult $Otx2^{flox/flox}$ mice, 14 days after single icv injection of vehicle (A–E) or CRE-Tat protein (F–J). Scale bar, 100 μm.

(K) Percentage of Otx2-, PV-, WFA-, CR-, and GABA-positive cells (CRE-Tat versus vehicle) in layers II–IV of V1b. Dashed line indicates vehicle-treated levels (t test, four mice per group; $^{**}p < 0.01$).

(L) Quantification of the mean intensity of Otx2, PV, CR, and GABA staining per cell in supragranular layers of V1b (t test, four mice per group; $^{**}p < 0.01$, $^{***}p < 0.001$; 700 × 450 μm area).

(M) Quantification of western blots of non-cell-autonomous Otx2 protein after vehicle or CRE-Tat injection in adult $Otx2^{flox/flox}$ mice (normalized with tubulin, mice 3–4 months old; t test; nine mice per group; $^{**}p < 0.01$).

(N) Quantification of western blots of non-cell-autonomous Otx2 protein in visual cortex during postnatal development (normalized with tubulin; t test, five WT mice for each age; $^{**}p < 0.01$).

(O) Quantification of *Otx2* mRNA content in the choroid plexus during postnatal development (relative to GAPDH, t test, six WT mice for each age; $^{*}p < 0.05$).

(P) Western blot of mCSF (150 μl per age, pooled from approximately ten mice) from pre- (P20) and post-CP (P45) time points. Exposure time for Otx2 was 200-fold longer than for TTR.

Error bars, SEM.

internalization during development and in the adult (Beurdeley et al., 2012; Miyata et al., 2012; Sugiyama et al., 2008).

Knocking Down *Otx2* in the Choroid Plexus Restores Plasticity in Visual Cortex

Downregulation of PV expression and PNN structures by direct blockade of Otx2 transfer into visual cortex induces a "juvenile" stage permissive for plasticity (Beurdeley et al., 2012). To test the functional impact of choroid-derived Otx2, we used visually evoked potential (VEP) recordings to measure visual acuity. In adult (>P90) wild-type mice, a short-term monocular deprivation (STMD; 4 days) fails to impair vision (Bavelier et al., 2010; Prusky and Douglas, 2003). In strong contrast, STMD imposed 2 weeks after a single CRE-Tat injection into the ventricles of adult $Otx2^{flox/flox}$ mice significantly decreased visual acuity, indicating a reactivation of cortical plasticity (Figures 4A, 4B, and S1; vehicle: 0.49 ± 0.02 versus CRE-Tat: 0.31 ± 0.03 cycles/degree; $p = 0.004$).

The therapeutic value of reducing choroid-derived Otx2 was further confirmed by monitoring recovery from amblyopia induced earlier in life. Ventricular CRE-Tat injection in adult $Otx2^{flox/flox}$ mice during the recovery period rescued visual acuity from an initial long-term deprivation spanning the CP (Figures 4C, 4D, and S1; vehicle: 0.26 ± 0.01 versus CRE-Tat: 0.38 ± 0.01 cycles/degree; $p = 0.0005$). These results are comparable to those obtained after direct blockade of Otx2 transfer within visual cortex (Beurdeley et al., 2012). Specific interactions between a sugar-binding motif in Otx2 and PNNs maintain a metastable physiological state of PV cells (Beurdeley et al., 2012; Miyata et al., 2012). Taken together, plasticity may be

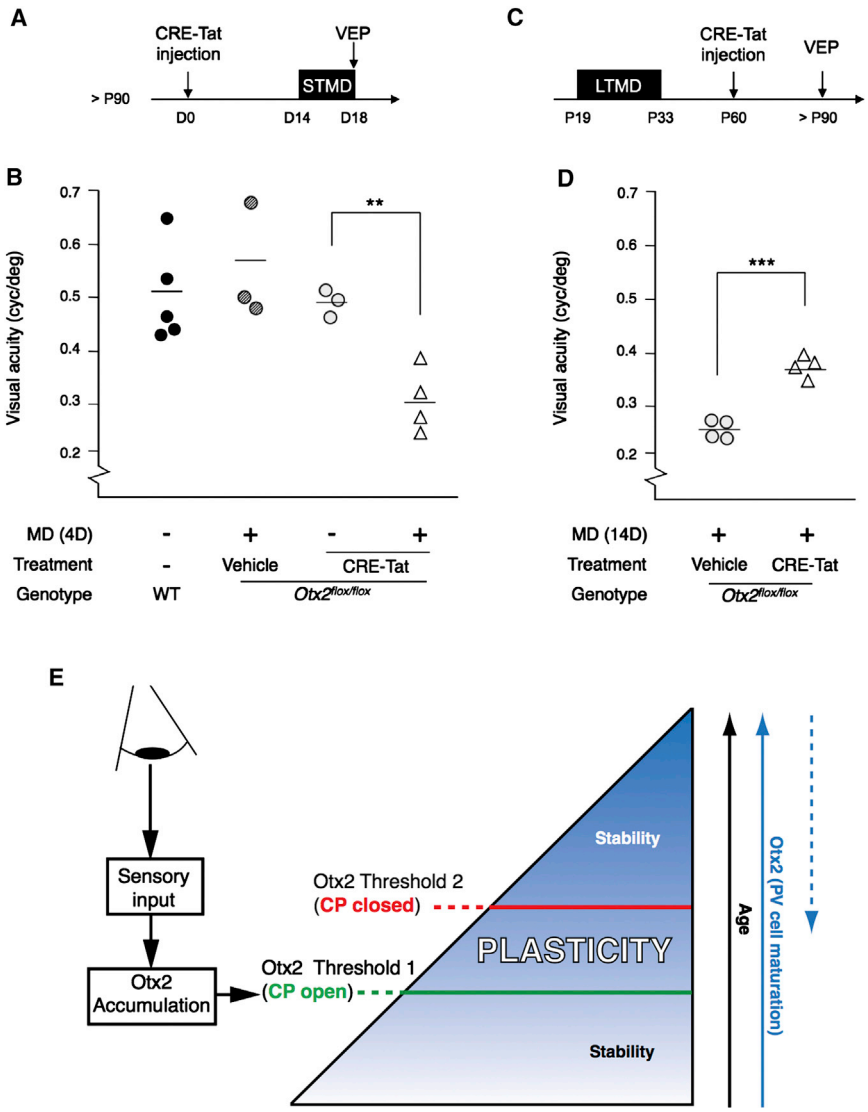

Figure 4. Choroid *Otx2* Disruption Reactivates Plasticity in Adult Visual Cortex

(A) Schematic of adult (>P90) visual cortical plasticity paradigm by short-tern (4 day) monocular deprivation.

(B) Visual acuity in untreated adult wild-type or $Otx2^{flox/flox}$ mice injected icv with either vehicle or CRE-Tat protein. Two weeks postinjection, $Otx2^{flox/flox}$ mice underwent STMD (or not) just before VEP recording. Horizontal bar indicates mean value for each group (t test; three to five mice per group; $^{**}p < 0.01$).

(C) Schematic of amblyopia-recovery paradigm. Amblyopia is induced during the CP via a long-term (14 days) monocular deprivation (LTMD). CRE-Tat injections are made 4 weeks after eye suture removal. VEP acuity is then measured in adulthood (>P90).

(D) Visual acuity recovers significantly in adult $Otx2^{flox/flox}$ mice injected icv with CRE-Tat protein (t test; four mice per group; $^{***}p < 0.001$).

(E) A two-threshold model for Otx2 regulation of cortical plasticity. Early sensory experience initiates the accumulation of Otx2 in PV cells to promote their functional maturation and plasticity onset. As the CP proceeds, PNNs condense tightly around these PV cells causing higher levels of Otx2 to accumulate and to structurally stabilize the local circuit. This process is reversible by knocking down Otx2 synthesis at its source in the choroid plexus (dashed arrow).

See also Figure S1.

activated at a low Otx2 threshold and then actively repressed in adulthood by the continuous transfer of choroid-derived Otx2 into mature PV cells after a second threshold has been passed. This model (Figure 4E) is discussed below.

DISCUSSION

In a previous study, we have shown that one allele of *Otx2* is not enough to induce plasticity in V1 (Sugiyama et al., 2008). Conversely, here, we demonstrate that reducing adult Otx2 content by only 32% is enough to reopen plasticity. This suggests a physiological range for Otx2 action defined by two thresholds (Figure 4E): one to open and another one to close plasticity. This is reminiscent of a "French flag" model of maturation similar to that proposed by Lewis Wolpert (Wolpert, 1969); here, a temporal model as the morphogen concentration increases with time within PV cells. Importantly, the second threshold is "reversible" because decreasing Otx2 concentration engages the plastic regime (this study; Beurdeley et al., 2012).

The model also stipulates that early sensory experience (sensory input) initiates expression of Otx2-binding sites on nascent PNNs (Beurdeley et al., 2012; Miyata et al., 2012), facilitating Otx2 import and opening a period of plasticity. Subsequent Otx2 internalization increases intracellular Otx2 and PV cell maturation reflected by further PV expression and PNN assembly (Sugiyama et al., 2008) until a second threshold is reached that closes plasticity. In support of the hypothesis is that direct infusion of Otx2 before CP opening opens CP ahead of time and also closes it ahead of time (Sugiyama et al., 2008). Moreover, the opening of plasticity (first threshold) does not take place in dark-reared animals, where the Otx2 and PV levels remain low in PV cells. Instead, PV cell maturation in dark-reared animals is rescued by direct Otx2 infusion leading to its specific accumulation in PV cells and CP opening (Sugiyama et al., 2008).

Together, this indicates that the ability of PV cells to capture Otx2 after initial PNN assembly may be the key event that regulates plasticity independently of age. This is further supported by the demonstration that the knockout of specific sulfotransferases that modify the PNN structure interferes with Otx2 internalization and CP closure (Miyata et al., 2012) and that the permanent transfer of Otx2 through PNN

recognition is necessary to repress plasticity in the adult (Beurdeley et al., 2012). The finding that hydrolysis of chondroitin sulfates reopens plasticity in the adult rat visual cortex may thus be explained, in part, by the persistent role of PNNs in Otx2 transport into PV cells (Pizzorusso et al., 2002). Overall, one can propose that plasticity during development and in the adult is regulated by Otx2 import and that PNNs are the gatekeepers of Otx2.

The source of Otx2 then becomes an important point to consider. Blocking Otx2 transport in the retina (between bipolar cells and retinal ganglion cells) or in the cortex (by directly infusing Otx2 antibodies) retards the activity-dependent opening of CP in the visual cortex (Sugiyama et al., 2008). The activity-dependent CP opening may thus require the transport of Otx2 along the visual pathway and ensuing initial maturation of PV cells marked by PNN assembly. Accordingly, we showed that Otx2 injected in the eye can travel along this pathway and terminates in PV cells (Sugiyama et al., 2008, 2009). It is also plausible that neural activity per se regulates PNN assembly through another mechanism and that Otx2 from other sources is internalized by the maturing PV cells.

The two possibilities are not mutually exclusive, and the most important point is that the first threshold (Figure 4E) is activity dependent. The observation that Otx2 is present in PV cells outside the visual cortex (Figure 1) favors a more general source, supported here by the choroid plexus. The activity-dependent opening of plasticity based on PNN assembly and Otx2 capture might explain why CPs do not open uniformly throughout the cortex even though the choroid plexus provides a continuous supply of Otx2. Salient patterns of neural input emerge at different times as the various peripheral sense organs come online. The same scheme also explains how a general source, thanks to mature, fully assembled PNNs, participates in maintaining a nonplastic state, allowing for the possibility to reopen plasticity in adulthood (Beurdeley et al., 2012; Pizzorusso et al., 2002).

Thus, one striking implication is that the choroid plexus, via the CSF, may be a general regulator of CP plasticity, including the amygdala (Gogolla et al., 2009), auditory (Barkat et al., 2011), or prefrontal cortex (Belforte et al., 2010; Yang et al., 2012)—structures with shifted or shorter CPs than V1. An important Otx2 target may be the enriched ATP metabolism in these fast-spiking cells (Plessy et al., 2008). Indeed, translation of nuclear-encoded mitochondrial mRNAs commonly follows homeoprotein capture by dopaminergic neurons or retinal ganglion cell growth cones (Alvarez-Fischer et al., 2011; Stettler et al., 2012; Yoon et al., 2012). Correspondingly, PV cells are highly vulnerable to oxidative stress across a number of cognitive disorders (Do et al., 2009), which may be protected by PNNs (Cabungcal et al., 2013).

The choroid plexus then offers an additional route to access brain plasticity through the peripheral blood supply (Johanson et al., 2008). For example, cell-permeable peptides injected into the retro-orbital sinus can efficiently deliver reagents (e.g., morpholinos, siRNA) to transiently knock down Otx2 synthesis in the choroid plexus (see Figure S2). The differential kinetics of Otx2 regulation across brain regions might then be paired effectively with therapeutic strategies for neurodevelopmental disorders more broadly.

EXPERIMENTAL PROCEDURES

Animals

Conventionally raised C57Bl/6 mice (12:12 hr light:dark cycle) were purchased from Janvier. ROSA26R reporter mice were obtained from The Jackson Laboratory. *Otx2*$^{flox/flox}$ mice were generated and kindly donated by Dr. T. Lamonerie (IBDC) (Fossat et al., 2006) and S Aizawa (RIKEN CDB) (Nishida et al., 2003). All procedures were designed to minimize animal suffering and carried out in accordance with the recommendations of the European Economic Community (86/609/EEC), the French National Committee (87/848) for the use of laboratory animals, and the IACUC committee of Boston Children's Hospital.

Cell Surface Biotinylation

Adult mouse choroid plexus from the lateral and fourth ventricles was rapidly extracted in PBS and immediately processed for biotinylation with EZlink-SulfoNHS-Biotin (Pierce; #21326) in PBS for 30 min at room temperature (RT) with gentle agitation. Following several washes, tissues were disrupted by sonication in the presence of protease inhibitors and nucleases. After clarification, the lysate was incubated with magnetic streptavidin beads (Dynabeads, #65001) for 20 min at 4°C. Following intensive washing, beads were directly resuspended in SDS-PAGE loading buffer, and eluted biotinylated proteins were processed for western blot detection with the indicated antibodies.

CSF Sampling

The CSF-sampling procedure was adapted from described methods by Liu and Duff (2008) and Morrey et al. (2008). Briefly, anesthetized mice were mounted on a stereotaxic frame, the dura covering the cisterna magna was gently exposed, and the surrounding area was thoroughly cleaned using sterile saline-soaked cotton swabs. CSF was mechanically aspirated through a 30G needle connected to a sterile polyvinylchloride catheter tube (ID, 0.69 mm; OD, 1.14 mm; Alzet) and inserted into the cisterna magna. On average, 15 μl of CSF could be sampled from an adult mouse. Any samples contaminated with the slightest traces of blood were discarded. During the collection procedure, CSF samples were kept on ice, in the presence of PMSF (1 mM). Prior to acetone-mediated total protein precipitation, CSF was subjected to centrifugation (for 1 min at 1,000 × *g* and then 20 min at 17,000 × *g*) to remove cells and cell fragments. The protein pellet was finally resuspended in SDS-PAGE loading buffer and processed for western blot detection.

Protein Production

The coding sequence of CRE-Tat protein was inserted in a derivative of pSCherry2 (Eurogentec) and expressed in SE1 cells grown in MagicMedia Medium (Invitrogen) according to manufacturer's instructions (details of the constructs available on request). Briefly, cells were grown for 18 hr at 37°C and then harvested by centrifugation. Pellets were frozen at −80°C. Bacteria were resuspended in buffer A (300 mM NaCl, 10 mM phosphate buffer, 30 mM imidazole [pH 7.5] with protease inhibitors; Roche Diagnostics) and disrupted by sonication (Bioruptor; Diagenode). The lysate was clarified by centrifugation (13,000 × *g*, 20 min, 4°C) and passed through a 0.45 μm filter. The protein was purified by two successive steps of affinity chromatography, first on Nickel column and second on heparin column following removal of the polyhistidine tag by preScisson proteolytic cleavage. The recombinant protein was eluted on FPLC (AKTA; GE Healthcare), with a linear gradient of NaCl (ranging from 0.3 to 2 M), in 10 mM phosphate buffer (pH 7.5). Fractions were quantified and analyzed on SDS-PAGE and stored at −20°C directly in the elution buffer.

Protein Injection

CRE-Tat recombinant protein (or vehicle) was injected bilaterally into the lateral ventricles of adult mice, using a 10 μl Hamilton syringe coupled to an electronic injection device, at a rate of 0.2 μl/min. Coordinates for injections were (with respect to bregma) −0.58 mm on the A/P axis, ±1.28 mm laterally, and 2 mm in depth. Five days after injection, injected ROSA26R reporter mice were perfused transcardially with PBS followed by 4% paraformaldehyde (PFA) prepared in PBS. After 4 hr of postfixation in 4% PFA, brains were washed in PBS. Coronal brain sections (50 μm) were cut on a vibratome

(Microm) and processed for X-Gal staining. *Otx2*$^{flox/flox}$ mice were sacrificed 2 weeks after injection. Following intracardiac PBS perfusion, the retina, choroid plexus (pooled lateral and fourth ventricles), dLGN, and SC were rapidly extracted in PBS, frozen on dry ice, and stored at −80°C. Cerebral cortices were left intact and further processed for immunostaining. To that end, tissues were fixed for 6 hr in 4% PFA, washed with PBS, and sliced on a vibratome. Alternatively, posterior cortex layer IV was dissected under a dissection microscope, frozen on dry ice, and stored at −80°C prior to total protein lysate preparation and western blot detection.

DNA, RNA, and Protein Extraction

Using the All Prep DNA/RNA Mini Kit (QIAGEN), genomic DNA, total RNA, and proteins could be simultaneously recovered from the same biological samples. Frozen choroid plexus, retina, dLGN, and SC were processed following manufacturer's instructions.

PCR

PCR was used to confirm the efficiency of CRE-induced recombination at the level of genomic DNA. To that end, we used C and E primers as previously described by Fossat et al. (2006). Because these primers hybridize on either side of the flox cassettes, excised and wild-type alleles could be distinguished by the size of the amplified fragments.

Quantitative RT-PCR

First-strand cDNA was synthesized using 100 ng of total mRNA, a blend of Omniscript and Sensiscript Reverse Transcriptases, and a mix of oligo-dT and random primers (QuantiTect Reverse Transcription Kit; QIAGEN). For real-time PCR, samples were analyzed in triplicate with a LightCycler 480 II (Roche). Gene-to-GAPDH ratios were determined using the $2^{-\Delta\Delta Ct}$ method.

Western Blot

Proteins from choroid plexus, retina, dLGN, SC, cortical layer IV, and CSF samples were separated on NuPAGE 4%–12% Bis-Tris precasted gels (Invitrogen) and transferred onto PVDF membrane. Primary antibodies were incubated overnight at 4°C and HRP-coupled secondary antibodies for 1 hr at RT. The following antibodies were used: anti-Otx2 (rat polyclonal, 1/20,00) (Sugiyama et al., 2008); anti α-tubulin (mouse monoclonal, clone B-5-1-2, 1/75,000; Sigma-Aldrich); anti RhoA (mouse monoclonal, clone 26CA, 1/500; Santa Cruz Biotechnology); anti-TTR (rabbit polyclonal, 1/2,000; Interchim); and anti-TrkB (rabbit monoclonal, clone 80E3, 1/1,000; CST). Corresponding HRP-coupled secondary antibodies were purchased from GE Healthcare (1/4,000–1/10,000).

In Situ Hybridization and Immunostaining

In situ hybridization was performed as described by Sugiyama et al. (2008). Briefly, 50 μm floating sections were hybridized overnight at 70°C with a digoxigenin (DIG)-labeled RNA probe for *Otx2* mRNA. The binding of the probe was revealed using an alkaline phosphatase (AP)-coupled DIG antibody (sheep polyclonal, 1/1,000; Roche Applied Science). For immunostaining, floating sections were incubated with primary antibodies overnight at 4°C, intensively washed at RT, and further incubated with corresponding Alexa Fluor-conjugated secondary antibodies overnight at 4°C. The following primary antibodies were used: anti-Otx2 (rat polyclonal, 1/200) (Sugiyama et al., 2008); anti-PV (mouse monoclonal, clone PARV-19, 1/400; Sigma-Aldrich); anti-Calretinin (rabbit serum, 1/2,000; Swant); and anti-GABA (rabbit polyclonal, 1/1,000; Sigma-Aldrich). Secondary antibodies were used as follows: anti-rat Alexa Fluor 561 (1/5,000; Molecular Probes); anti-Mouse Alexa Fluor 488 (1/5,000; Molecular Probes); and anti-Rabbit Alexa Fluor 633 (1/5,000; Molecular Probes). Biotinylated-WFA was purchased from Sigma-Aldrich (1/100) and was detected by means of Alexa Fluor 633-conjugated streptavidin (Molecular Probes). Stained sections were mounted in Fluoromount medium (SouthernBiotech), and images were acquired using a Leica SP5 confocal microscope.

VEPs

Electrophysiological recordings were performed under Nembutal/chlorprothixene anesthesia using standard techniques (Beurdeley et al., 2012). Transient VEPs in response to abrupt contrast reversal (100%, 1 Hz) over a range of spatial frequencies (0.01–0.6 cycles/degree) were band-pass filtered (0.1–100 Hz), amplified, and fed to a computer for analysis. In brief, at least 20 events were averaged in synchrony with the stimulus contrast reversal. Visual acuity was obtained by extrapolation to zero amplitude after correction of noise level. Monocular deprivation consisted of eyelid suture under isoflurane anesthesia; in some cases, the suture was reopened to test for recovery.

SUPPLEMENTAL INFORMATION

Supplemental Information includes two figures and can be found with this article online at http://dx.doi.org/10.1016/j.celrep.2013.05.014.

LICENSING INFORMATION

ACKNOWLEDGMENTS

We thank Professor M. Volovitch for useful discussions. In addition to institutional support, this study was funded by grants to A.J. and A.P. from the Agence Nationale pour la Recherche (ANR-10-BLAN-141-01 and ANR-11-BLAN-069467), the Global Research Laboratory Program (2009-00424) from the Korean Ministry of Education, Science and Technology, and the Region Ile de France. T.K.H. was supported by NIH (1 DP1 OD 003699) and by NIMH (5P50MH094271), J.S. was a College de France Post-Doctoral Fellow, and H.H.C.L. was a Croucher Foundation (Hong Kong) Fellow.

Received: August 2, 2012
Revised: March 26, 2013
Accepted: May 9, 2013
Published: June 13, 2013

REFERENCES

Alonso, M.I., Martín, C., Carnicero, E., Bueno, D., and Gato, A. (2011). Cerebrospinal fluid control of neurogenesis induced by retinoic acid during early brain development. Dev. Dyn. *240*, 1650–1659.

Alvarez-Fischer, D., Fuchs, J., Castagner, F., Stettler, O., Massiani-Beaudoin, O., Moya, K.L., Bouillot, C., Oertel, W.H., Lombès, A., Faigle, W., et al. (2011). Engrailed protects mouse midbrain dopaminergic neurons against mitochondrial complex I insults. Nat. Neurosci. *14*, 1260–1266.

Barkat, T.R., Polley, D.B., and Hensch, T.K. (2011). A critical period for auditory thalamocortical connectivity. Nat. Neurosci. *14*, 1189–1194.

Bavelier, D., Levi, D.M., Li, R.W., Dan, Y., and Hensch, T.K. (2010). Removing brakes on adult brain plasticity: from molecular to behavioral interventions. J. Neurosci. *30*, 14964–14971.

Belforte, J.E., Zsiros, V., Sklar, E.R., Jiang, Z., Yu, G., Li, Y., Quinlan, E.M., and Nakazawa, K. (2010). Postnatal NMDA receptor ablation in corticolimbic interneurons confers schizophrenia-like phenotypes. Nat. Neurosci. *13*, 76–83.

Beurdeley, M., Spatazza, J., Lee, H.H., Sugiyama, S., Bernard, C., Di Nardo, A.A., Hensch, T.K., and Prochiantz, A. (2012). Otx2 binding to perineuronal nets persistently regulates plasticity in the mature visual cortex. J. Neurosci. *32*, 9429–9437.

Cabungcal, J.H., Steullet, P., Morishita, H., Kraftsik, R., Cuenod, M., Hensch, T.K., and Do, K.Q. (2013). Perineuronal nets protect fast-spiking interneurons against oxidative stress. Proc. Natl. Acad. Sci. USA *110*, 9130–9135.

Di Lullo, E., Haton, C., Le Poupon, C., Volovitch, M., Joliot, A., Thomas, J.L., and Prochiantz, A. (2011). Paracrine Pax6 activity regulates oligodendrocyte precursor cell migration in the chick embryonic neural tube. Development *138*, 4991–5001.

Do, K.Q., Cabungcal, J.H., Frank, A., Steullet, P., and Cuenod, M. (2009). Redox dysregulation, neurodevelopment, and schizophrenia. Curr. Opin. Neurobiol. *19*, 220–230.

Elbert, T., Pantev, C., Wienbruch, C., Rockstroh, B., and Taub, E. (1995). Increased cortical representation of the fingers of the left hand in string players. Science *270*, 305–307.

Fossat, N., Chatelain, G., Brun, G., and Lamonerie, T. (2006). Temporal and spatial delineation of mouse Otx2 functions by conditional self-knockout. EMBO Rep. *7*, 824–830.

Gogolla, N., Caroni, P., Lüthi, A., and Herry, C. (2009). Perineuronal nets protect fear memories from erasure. Science *325*, 1258–1261.

Hensch, T.K. (2004). Critical period regulation. Annu. Rev. Neurosci. *27*, 549–579.

Hensch, T.K. (2005). Critical period plasticity in local cortical circuits. Nat. Rev. Neurosci. *6*, 877–888.

Huang, X., Liu, J., Ketova, T., Fleming, J.T., Grover, V.K., Cooper, M.K., Litingtung, Y., and Chiang, C. (2010). Transventricular delivery of Sonic hedgehog is essential to cerebellar ventricular zone development. Proc. Natl. Acad. Sci. USA *107*, 8422–8427.

Johanson, C.E., Duncan, J.A., 3rd, Klinge, P.M., Brinker, T., Stopa, E.G., and Silverberg, G.D. (2008). Multiplicity of cerebrospinal fluid functions: new challenges in health and disease. Cerebrospinal Fluid Res. *5*, 10.

Johansson, P.A., Irmler, M., Acampora, D., Beckers, J., Simeone, A., and Götz, M. (2013). The transcription factor Otx2 regulates choroid plexus development and function. Development *140*, 1055–1066.

Koike, C., Nishida, A., Ueno, S., Saito, H., Sanuki, R., Sato, S., Furukawa, A., Aizawa, S., Matsuo, I., Suzuki, N., et al. (2007). Functional roles of Otx2 transcription factor in postnatal mouse retinal development. Mol. Cell. Biol. *27*, 8318–8329.

Kuhl, P.K., Williams, K.A., Lacerda, F., Stevens, K.N., and Lindblom, B. (1992). Linguistic experience alters phonetic perception in infants by 6 months of age. Science *255*, 606–608.

Lehtinen, M.K., Zappaterra, M.W., Chen, X., Yang, Y.J., Hill, A.D., Lun, M., Maynard, T., Gonzalez, D., Kim, S., Ye, P., et al. (2011). The cerebrospinal fluid provides a proliferative niche for neural progenitor cells. Neuron *69*, 893–905.

Liu, L., and Duff, K. (2008). A technique for serial collection of cerebrospinal fluid from the cisterna magna in mouse. J. Vis. Exp. (21), pii: 960.

Martín, C., Bueno, D., Alonso, M.I., Moro, J.A., Callejo, S., Parada, C., Martín, P., Carnicero, E., and Gato, A. (2006). FGF2 plays a key role in embryonic cerebrospinal fluid trophic properties over chick embryo neuroepithelial stem cells. Dev. Biol. *297*, 402–416.

Maurer, D., and Hensch, T.K. (2012). Amblyopia: background to the special issue on stroke recovery. Dev. Psychobiol. *54*, 224–238.

Miyata, S., Komatsu, Y., Yoshimura, Y., Taya, C., and Kitagawa, H. (2012). Persistent cortical plasticity by upregulation of chondroitin 6-sulfation. Nat. Neurosci. *15*, 414–422, S1–S2.

Morrey, J.D., Olsen, A.L., Siddharthan, V., Motter, N.E., Wang, H., Taro, B.S., Chen, D., Ruffner, D., and Hall, J.O. (2008). Increased blood-brain barrier permeability is not a primary determinant for lethality of West Nile virus infection in rodents. J. Gen. Virol. *89*, 467–473.

Nelson, C.A., 3rd, Zeanah, C.H., Fox, N.A., Marshall, P.J., Smyke, A.T., and Guthrie, D. (2007). Cognitive recovery in socially deprived young children: the Bucharest Early Intervention Project. Science *318*, 1937–1940.

Nishida, A., Furukawa, A., Koike, C., Tano, Y., Aizawa, S., Matsuo, I., and Furukawa, T. (2003). Otx2 homeobox gene controls retinal photoreceptor cell fate and pineal gland development. Nat. Neurosci. *6*, 1255–1263.

Nothias, F., Fishell, G., and Ruiz i Altaba, A. (1998). Cooperation of intrinsic and extrinsic signals in the elaboration of regional identity in the posterior cerebral cortex. Curr. Biol. *8*, 459–462.

Pizzorusso, T., Medini, P., Berardi, N., Chierzi, S., Fawcett, J.W., and Maffei, L. (2002). Reactivation of ocular dominance plasticity in the adult visual cortex. Science *298*, 1248–1251.

Plessy, C., Fagiolini, M., Wagatsuma, A., Harasawa, N., Kuji, T., Asaka-Oba, A., Kanzaki, Y., Fujishima, S., Waki, K., Nakahara, H., et al. (2008). A resource for transcriptomic analysis in the mouse brain. PLoS One *3*, e3012.

Prusky, G.T., and Douglas, R.M. (2003). Developmental plasticity of mouse visual acuity. Eur. J. Neurosci. *17*, 167–173.

Puelles, E., Annino, A., Tuorto, F., Usiello, A., Acampora, D., Czerny, T., Brodski, C., Ang, S.L., Wurst, W., and Simeone, A. (2004). Otx2 regulates the extent, identity and fate of neuronal progenitor domains in the ventral midbrain. Development *131*, 2037–2048.

Rath, M.F., Muñoz, E., Ganguly, S., Morin, F., Shi, Q., Klein, D.C., and Møller, M. (2006). Expression of the Otx2 homeobox gene in the developing mammalian brain: embryonic and adult expression in the pineal gland. J. Neurochem. *97*, 556–566.

Rath, M.F., Morin, F., Shi, Q., Klein, D.C., and Møller, M. (2007). Ontogenetic expression of the Otx2 and Crx homeobox genes in the retina of the rat. Exp. Eye Res. *85*, 65–73.

Sawamoto, K., Wichterle, H., Gonzalez-Perez, O., Cholfin, J.A., Yamada, M., Spassky, N., Murcia, N.S., Garcia-Verdugo, J.M., Marin, O., Rubenstein, J.L., et al. (2006). New neurons follow the flow of cerebrospinal fluid in the adult brain. Science *311*, 629–632.

Simeone, A., Acampora, D., Mallamaci, A., Stornaiuolo, A., D'Apice, M.R., Nigro, V., and Boncinelli, E. (1993). A vertebrate gene related to orthodenticle contains a homeodomain of the bicoid class and demarcates anterior neuroectoderm in the gastrulating mouse embryo. EMBO J. *12*, 2735–2747.

Soriano, P. (1999). Generalized lacZ expression with the ROSA26 Cre reporter strain. Nat. Genet. *21*, 70–71.

Stettler, O., Joshi, R.L., Wizenmann, A., Reingruber, J., Holcman, D., Bouillot, C., Castagner, F., Prochiantz, A., and Moya, K.L. (2012). Engrailed homeoprotein recruits the adenosine A1 receptor to potentiate ephrin A5 function in retinal growth cones. Development *139*, 215–224.

Sugiyama, S., Di Nardo, A.A., Aizawa, S., Matsuo, I., Volovitch, M., Prochiantz, A., and Hensch, T.K. (2008). Experience-dependent transfer of Otx2 homeoprotein into the visual cortex activates postnatal plasticity. Cell *134*, 508–520.

Sugiyama, S., Prochiantz, A., and Hensch, T.K. (2009). From brain formation to plasticity: insights on Otx2 homeoprotein. Dev. Growth Differ. *51*, 369–377.

Timmusk, T., Mudò, G., Metsis, M., and Belluardo, N. (1995). Expression of mRNAs for neurotrophins and their receptors in the rat choroid plexus and dura mater. Neuroreport *6*, 1997–2000.

Weisner, B., and Roethig, H.J. (1983). The concentration of prealbumin in cerebrospinal fluid (CSF), indicator of CSF circulation disorders. Eur. Neurol. *22*, 96–105.

Wizenmann, A., Brunet, I., Lam, J.S.Y., Sonnier, L., Beurdeley, M., Zarbalis, K., Weisenhorn-Vogt, D., Weinl, C., Dwivedy, A., Joliot, A., et al. (2009). Extracellular Engrailed participates in the topographic guidance of retinal axons in vivo. Neuron *64*, 355–366.

Wolpert, L. (1969). Positional information and the spatial pattern of cellular differentiation. J. Theor. Biol. *25*, 1–47.

Yang, E.J., Lin, E.W., and Hensch, T.K. (2012). Critical period for acoustic preference in mice. Proc. Natl. Acad. Sci. USA *109*(*Suppl 2*), 17213–17220.

Yoon, B.C., Jung, H., Dwivedy, A., O'Hare, C.M., Zivraj, K.H., and Holt, C.E. (2012). Local translation of extranuclear lamin B promotes axon maintenance. Cell *148*, 752–764.

Cell PRESS
Open ACCESS

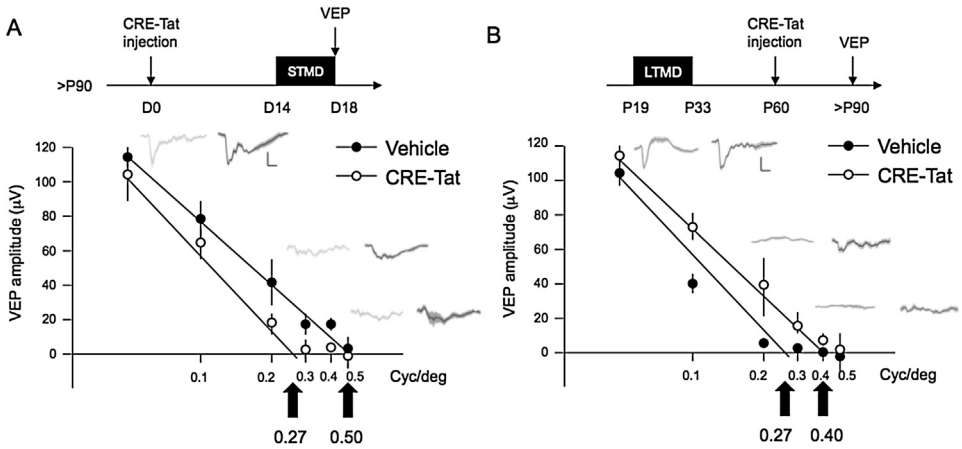

Figure S1. Visual Acuity after Choroid *Otx2* Disruption, Related to Figure 4

(A) Representative VEP average amplitudes (mean ± SEM) at different spatial frequencies (0.05 – 0.5 cyc/deg) after STMD coupled with CRE-Tat (open circle) or vehicle (closed circle) injections in adult mice (>P90). Threshold acuity for each mouse is indicated by upward arrows on the graph. Sample VEP traces at 0.05, 0.2 and 0.4 cyc/deg are shown (scale: 50 μV, 0.1 s). Lighter traces, from a CRE-Tat-injected mouse; bolder traces, from a vehicle-injected mouse. Experimental timeline in days (D) is shown on top.

(B) Representative VEP average amplitudes (mean ± SEM) at different spatial frequencies (0.05 – 0.5 cyc/deg) after long-term deprivation (LTMD) spanning the critical period (P19 – P33) (Beurdeley et al., 2012), followed by CRE-Tat (open circle) or vehicle (closed circle) injections during binocular recovery at P60. Threshold acuity for each mouse is indicated by upward arrows on the graph. Sample VEP traces at 0.05, 0.2 and 0.4 cyc/deg are shown (scale: 50 μV, 0.1 s). Lighter traces, a vehicle-injected mouse; bolder traces, a CRE-Tat-injected mouse. Experimental paradigm is shown on top.

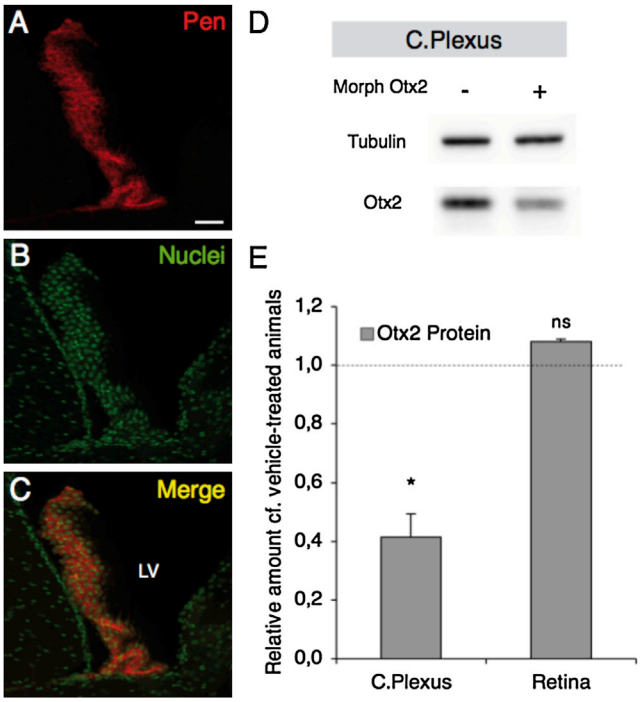

Figure S2. Noninvasive Route for Targeting Choroid Plexus Otx2, Related to Discussion

(A–C) Specific localization in the choroid plexus of a fluorescent version of the small peptide Penetratin (A,C; Pen-TAMRA, 100 μg), 15 min after injection into the retro-orbital sinus of adult mice. Nuclei are counterstained using SYBR Green (B, C). Scale bar: 50 μm. LV, Lateral Ventricle.

(D) Western Blot detection of Otx2 and tubulin protein in total choroid plexus extracts from mice injected in the retro-orbital sinus with either a vehicle solution (-) or a cell-permeable morpholino (Vivo-Morpholino, *Gene Tools, LLC*) directed against *Otx2* mRNA (+). 18 nmol of morpholino solution was injected once a day over two consecutive days. Mice were sacrificed 24 hr after the last injection.

(E) Quantification of Otx2 protein content in choroid plexus and retina of morpholino-treated animals compared to vehicle-treated controls (dashed line). Error bars, SEM (paired t test; 3 mice per group; *$p < 0.05$).